Geophysical Research Letters

Supporting Information for

Sustained growth of the Southern Ocean carbon storage in a warming climate

Takamitsu Ito[1*], Annalisa Bracco[1], Curtis Deutsch[2], Hartmut Frenzel[2], Matthew Long[3] and Yohei Takano[1]

1. School of Earth and Atmospheric Sciences, Georgia Institute of Technology, Atlanta, Georgia, U.S.A.
2. School of Oceanography, University of Washington, Seattle, Washington, U.S.A.
3. Climate and Global Dynamics Division, National Center for Atmospheric Research, Boulder, Colorado, U.S.A.

Contents of this file

Introduction

This document includes technical notes on:

1. Decomposition of dissolved inorganic carbon into preformed and regenerated components
2. Description of the ocean circulation and biogeochemistry model
3. A box model for the age of Circumpolar Deep Water
4. Table of CMIP5 model centers and model names

Text S1. Decomposition of dissolved inorganic carbon into preformed and regenerated components

The dissolved inorganic carbon present in the seawater can be separated into two components: (1) preformed carbon which was present at the time when the water was in last contact with the atmosphere, and (2) regenerated carbon which has been regenerated from dissolution of organic matter and calcium carbonate particles. To quantify the partitioning between the preformed and regenerated pool of carbon, the oxidative component of regenerated carbon is estimated using the apparent oxygen utilization multiplied by the carbon to oxygen stoichiometric ratio. The carbonate component of regenerated carbon is also estimated using the apparent alkalinity regeneration multiplied by the factor of one half.

To apply this concept to the CMIP-5 models, we use the stoichiometric ratios in respective model based on the published values. N:P ratio assumed to be 16 in all models. For GFDL, NCAR and Hadley center models, we assume 106 for C:P and 150 for O_2:P ratios. For IPSL and MPI models, we assume 122 for C:P and 172 for O_2:P ratios. However, N:P ratio and C:P ratio may vary depending on the dominant phytoplankton type and physiological response to local environment. This is likely a secondary effect but it is a source of uncertainty in this analysis. To calculate the apparent alkalinity regeneration, we estimate the preformed alkalinity as a linear function of salinity by performing regression analysis.

Our decomposition in CMIP-5 models is also subject to uncertainties associated with the ability of the apparent oxygen utilization and apparent alkalinity regeneration to account for the regeneration of carbon and the effect of air-sea disequilibrium. The air-sea disequilibrium responds to heat flux, entrainment and biological uptake that are difficult to diagnose without an additional diagnostic tracer. Generally, there is a slightly positive preformed AOU (oxygen undersaturation) leading to an overestimation of regenerated carbon. In our GCM simulation, we explicitly simulate preformed tracers for carbon, alkalinity, oxygen and phosphorus and there is no uncertainty in the decomposition.

Text S2. Description of the ocean circulation and biogeochemistry model

We use the Massachusetts Institute of Technology general circulation model (MITgcm) [Marshall et al., 1997a; Marshall et al., 1997b] with a biogeochemistry component [Parekh et al., 2005] configured for a global bathymetry in 2.8°x2.8° longitude-latitude grid, and 23 non-uniform vertical levels. Mesoscale eddies are parameterized using the isopycnal thickness diffusion scheme [Gent and McWilliams, 1990] and the mixed-layer processes are parameterized using the K-Profile Parameterization scheme [Large et al., 1994]. The model carries dissolved inorganic carbon, alkalinity, phosphorus, dissolved organic phosphorus, iron, dissolved oxygen, preformed oxygen, preformed carbon, preformed alkalinity and ideal age as tracers. Biological productivity is controlled by the availability of light and nutrients (P or Fe) using a Monod function formulation. A similar configuration has been adopted in Parekh et al. [2005]. Here however we a use much higher vertical resolution near the surface for a better representation of the role of stratification in controlling the productivity.

The MITgcm does not account for the effects of iron availability on photosynthetic efficiency, while some CMIP-5 models do. In this model, the low iron level is limiting the productivity of the Southern Ocean during the productive summer seasons. Therefore the iron-light co-limitation effect plays a secondary role. Also, it has been shown in Galbraith et al. [2010] that differences in the simulation of global-scale biogeochemistry between models that account for the coupling between iron and light availability and models that neglect it are small.

Preformed properties allow us to diagnose the carbon pump components accurately [Ito and Follows, 2005]. The model is spun up with climatological wind stress, freshwater flux, and heat flux fields [Jiang et al., 1999; Trenberth et al., 1989]. A Newtonian relaxation is also applied to the sea surface temperature and salinity towards monthly climatology [Levitus et al., 1994ab]. Due to the lack of sea-ice/ice-shelf interactions and highly smoothed topography, the model cannot adequately form the Antarctic Bottom Water. To address this issue, climatological salinity in the polar Southern Ocean is locally raised to increase the deep ventilation there. This modification in the salinity restoring accelerates the lower overturning circulation, and oxygenates the abyssal Southern Ocean in much better agreement with observations. The global meridional overturning streamfunction from the control simulation is shown in figure S1.

After spinning up the model for several millennia to achieve a statistical steady state, we perform the perturbation experiments. The climate forcing patterns are motivated by the CMIP-5 simulations. Concurrent climate changes under rising atmospheric CO2 are increasing oceanic heat content (Heat), increasing freshwater fluxes, that is enhancing precipitation in the tropics and high-latitudes and increasing evaporation in the subtropics (EmP), and intensification and poleward-shifting of the Southern Ocean zonal wind. The forcing patterns and amplitudes are broadly based on the analysis of Capotondi et al., [2012] and are implemented in the sensitivity runs as listed below.

(Heat) Sea surface temperature is subject to a global uniform increase of 1°C per century
(EmP) Fresh water flux are intensified by 10% per century
(Wind) The zonal wind stress is intensified by approximately 10% and migrates poleward by 1°latitude per century
(All) All forcing patterns are included

The warming perturbation (Heat) is implemented by increasing the restoring boundary temperature in addition to the climatological sea surface temperature distribution. The freshwater perturbation (EmP) is implemented by globally modulating the amplitude of the monthly evaporation minus precipitation field while retaining its spatial pattern. Similar to the temperature, the freshwater forcing is imposed in addition to the climatological restoring. The SAM-based wind stress perturbation (Wind) is implemented by adding anomalies to the climatological wind stress. The anomalies are calculated using the regression coefficients based on the normalized monthly SAM index and monthly NCEP-1 reanalysis wind stress [Kalnay et al., 1996]. The resulting westerly wind stress intensifies approximately 10% per century and migrates poleward by 1°latitude per century.

Reference

Galbraith, E. D., A. Gnanadesikan, J. P. Dunne, and M. R. Hiscock (2010), Regional impacts of iron-light colimitation in a global biogeochemical model, Biogeosciences, 7, 1043–1064, doi: www.biogeosciences.net/7/1043/2010/

Gent, P. R., and J. C. McWilliams (1990), Isopycnal Mixing in Ocean Circulation Models, J Phys Oceanogr, 20(1), 150-155.

Ito, T., and M. J. Follows (2005), Preformed phosphate, soft tissue pump and atmospheric CO2, Journal of Marine Research, 63(4), 813-839, doi:10.1357/0022240054663231.

Jiang, S., P. H. Stone, and P. Malanotte-Rizzoli (1999), An assessment of the Geophysical Fluid Dynamics Laboratory ocean model with coarse resolution: Annual-mean climatology, J Geophys Res-Oceans, 104(C11), 25623-25645, doi:10.1029/1999jc900095.

Kalnay, E., et al. (1996), The NCEP/NCAR 40-Year Reanalysis Project, Bulletin of the American Meteorological Society, 77(3), 437-471.

Large, W. G., J. C. Mcwilliams, and S. C. Doney (1994), Oceanic Vertical Mixing - a Review and a Model with a Nonlocal Boundary-Layer Parameterization, Rev Geophys, 32(4), 363-403, doi:Doi 10.1029/94rg01872.

Levitus, S., R. Burgett, T. Boyer (1994a) World Ocean Atlas 1994, Vol. 3: Salinity. NOAA Atlas NESDIS 3,U.S. Gov. Printing Office, Wash., D.C., 99 pp.

Levitus, S., T. Boyer (1994b) World Ocean Atlas 1994, Vol. 4: Temperature. NOAA Atlas NESDIS 4, U.S. Gov. Printing Office, Wash., D.C., 117 pp.

Marshall, J., A. Adcroft, C. Hill, L. Perelman, and C. Heisey (1997a), A finite-volume, incompressible Navier Stokes model for studies of the ocean on parallel computers, J Geophys Res-Oceans, 102(C3), 5753-5766, doi:Doi 10.1029/96jc02775.

Marshall, J., C. Hill, L. Perelman, and A. Adcroft (1997b), Hydrostatic, quasi-hydrostatic, and nonhydrostatic ocean modeling, J Geophys Res-Oceans, 102(C3), 5733-5752, doi: 10.1029/96jc02776.

Parekh, P., M. J. Follows, and E. A. Boyle (2005), Decoupling of iron and phosphate in the global ocean, Global Biogeochem Cy, 19(2), GB2020, doi:10.1029/2004GB002280.

Trenberth, K. E., W. G. Large, and J. G. Olson (1989), The Effective Drag Coefficient for Evaluating Wind Stress over the Oceans, J Climate, 2(12), 1507-1516.

Text S3. A box model for the age of Circumpolar Deep Water

To illustrate the link between the two meridional overturning cells and the age of the Circumpolar Deep Water (CDW), we developed a simple box model to simulate the ideal age tracer. The deep Southern Ocean box represents the bulk of deep water masses south of 40°S below 400m including CDW and newly formed Antarctic Bottom Water (AABW). We assume that the two overturning cells together pull in deep waters with age of τ_N from the northern basins. When the deep water upwells to the surface box, its age is immediately set to zero, and subsequent sinking brings the surface water to the deep Southern Ocean. Thus the governing equation for the age of deep Southern Ocean is

$$V\frac{\partial \tau}{\partial t} = -\tau(\Psi_U + 2\Psi_L) + \tau_N(\Psi_U + \Psi_L) + V.$$

Then the equilibrium solution for the age of the deep Southern Ocean box is

$$\tau = \frac{(\Psi_U + \Psi_L)\tau_N + V}{\Psi_U + 2\Psi_L}$$

where Ψ_U and Ψ_L (m^3s^{-1}) are the volume flux of the upper and lower overturning circulations and V is the volume of the deep Southern Ocean box.

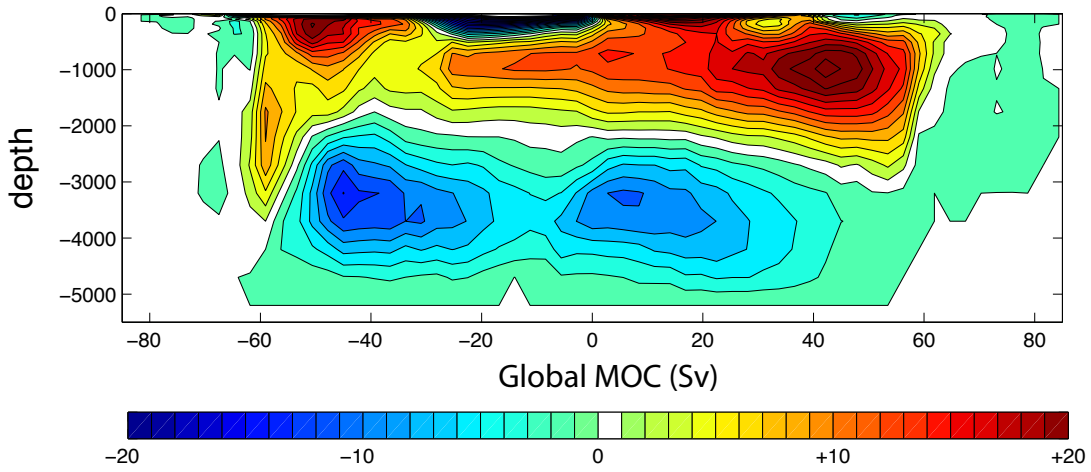

Figure S1. Simulated global meridional overturning circulation from the control simulation. Contour interval is 2Sv.

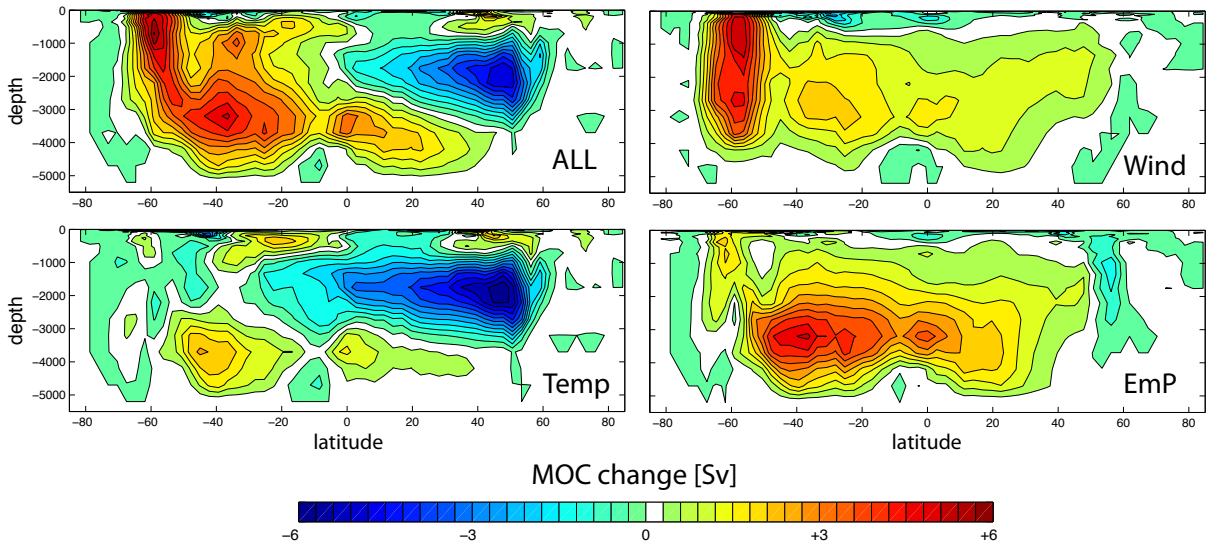

Figure S2. Sensitivities of the meridional overturning circulation to a warming climate. The change in the streamfunction is calculated by taking the difference between the perturbed simulation and the control simulation, evaluated at year 2100 (200 year perturbation). Contour interval is 0.5Sv.

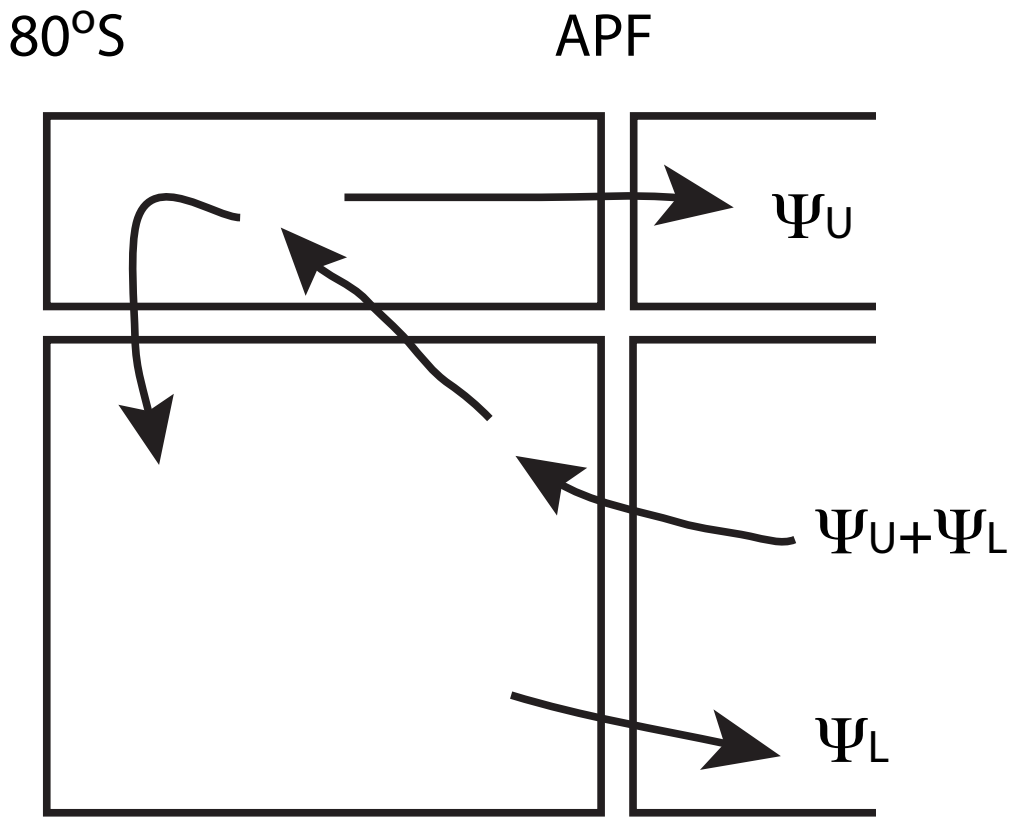

Figure S3. Box model for the age of the circumpolar deep water. The age of the incoming deep water from the northern basin, $\tau_{N,}$ is set to 250 years and the volume of the deep Southern ocean V is set to 2.78 x 10^{17} m^3.

Modeling group/center	Institute ID	Model name
NOAA Geophysical Fluid Dynamics Laboratory	NOAA GFDL	GFDL ESM2M GFDL ESM2G
Institut Pierre-Simon Laplace	IPSL	IPSL CM5A LR IPSL CM5A MR IPSL CM5B LR
Met Office Hadley Centre (additional HadGEM2-ES realizations contributed by Instituto Nacional de Pesquisas Espaciais)	MOHC (additional realizations by INPE)	HadGEM2-CC HadGEM2-ES
Max-Planck-Institut für Meteorologie (Max Planck Institute for Meteorology)	MPI-M	MPI-ESM-LR
Community Earth System Model Contributors	NSF-DOE-NCAR	CESM1(BGC)

Table S1. CMIP5 modeling groups and model names